DTU Library

Noise mapping inside a car cabin

Knudsen, Kim; Sjøj, Sidsel Marie Nørholm; Jacobsen, Finn; Haddad, Karim; Hald, Jørgen

Publication date:
2012

Document Version
Publisher's PDF, also known as Version of record

[Link back to DTU Orbit](#)

Noise mapping inside a car cabin

Sidsel Marie Nørholm Sjøj and Finn Jacobsen

Acoustic Technology, Department of Electrical Engineering, Technical University of Denmark, Ørsteds Plads, Building 352, DK-2800 Kgs. Lyngby, sidselmarie@gmail.com / fja@elektro.dtu.dk

Kim Knudsen

Department of Mathematics, Technical University of Denmark, Matematiktorvet, Building 303 S, DK-2800 Kgs. Lyngby, k.knudsen@mat.dtu.dk

Karim Haddad and Jørgen Hald

Brüel og Kjær Sound and Vibration A/S, Skodsborgvej 307, DK-2850 Nærum, Karim.Haddad@bksv.com / Jorgen.Hald@bksv.com

The mapping of noise is of considerable interest in the car industry where a good noise mapping can make it much easier to identify the sources that generate the noise and eventually reduce the individual contributions to the noise. The methods used for this purpose include delay-and-sum beamforming and spherical harmonics beamforming. These methods have a poor spatial esolution at low frequencies, and since much noise generated in cars is dominated by low frequencies the methods are not optimal. In the present paper the mapping is done by solving an inverse problem with a transfer matrix between the volume velocities of the sources and the measured sound pressures at the microphone array. This is an ill-posed problem and therefore regularisation have to be applied when the transfer matrix is inverted in order to give good results.

1   Introduction

Mapping of sound fields is of interest in many different areas. In the car industry mapping of noise sources is the first step towards reducing the output of the noise source and thereby increasing the comfort of the driver. Different methods can be used to map the sound field. Some of the methods used for this purpose are nearfield acoustic holography (NAH) and beamforming techniques using spherical arrays.

With NAH the measurement plane has to be very close to the source plane in order to catch the evanescent waves of the sound field and the spatial resolution is decreased with the distance between the planes. Mapping the sound field on the entire surface of a car cabin is therefore very time consuming because many measurements covering only small parts of the surface have to be done and added to give the full picture. On the other hand, NAH can give a mapping of very good resolution.

Beamforming techniques have the advantage that the measurements can be made further away from the source covering the entire sound field in a single measurement. However, the resolution is very poor at low frequencies even though it is improved with spherical harmonics beamforming instead of delay-and-sum beamforming. Since most noise generated by a car is dominated by low frequencies a good spatial resolution in this frequency range would be of interest. Moreover, spherical harmonics beamforming is not very good at reconstructing correlated sources. In a car cabin there will be many correlated sources because the enclosure is quite small and with many hard surfaces giving rise to many reflections that will be correlated with the primary source.

Because of these limitations it might be worthwhile to investigate alternative methods for the localisation of noise sources. Lamotte *et al.* [1] have reconstructed a sound field by inversion of a matrix problem describing the relation between a set of virtual sources and the sound pressures measured by a spherical microphone array and found interesting results. In the present paper the method is investigated further through simulations and measurements with respect to the spatial resolution under different conditions. The dependence of the distance between microphone array

and the sources and the signal-to-noise ratio (SNR) is studied through simulations, and the influence of different measurement conditions are studied by measurements in an anechoic chamber and in a box made of wood with varying amounts of absorbing panels applied to the walls.

Section 2 introduces the theoretical background of the problem. In Section 3 the results from simulations and measurements are presented followed by a discussion and conclusions in Sections 4 and 5. At the end some suggestions for future work are given in Section 6.

2   Outline of theory

2.1   Measurement model

The source distribution on the car cabin is found by solving a problem of the type

$$\mathbf{p} = \mathbf{Hq} \tag{1}$$

for the vector $\mathbf{q}$ containing volume velocities from n virtual sources on the car cabin [2]. The vector $\mathbf{p}$ contains the measured sound pressures from m microphones mounted on a rigid sphere ($m < n$), and $\mathbf{H}$ is an m by n transfer matrix between $\mathbf{q}$ and $\mathbf{p}$. Each element in $\mathbf{H}$ describes the relation between one virtual source and the corresponding sound pressure measured by one of the microphones. The elements of $\mathbf{H}$ can be found by solving the wave equation with appropriate boundary conditions, but since there is no analytical solution to this problem an assumption of free field conditions is made. This means that the true sources and the reflections due to the influence of the car cabin are represented by virtual sources distributed in a free field as illustrated in Figure 1.
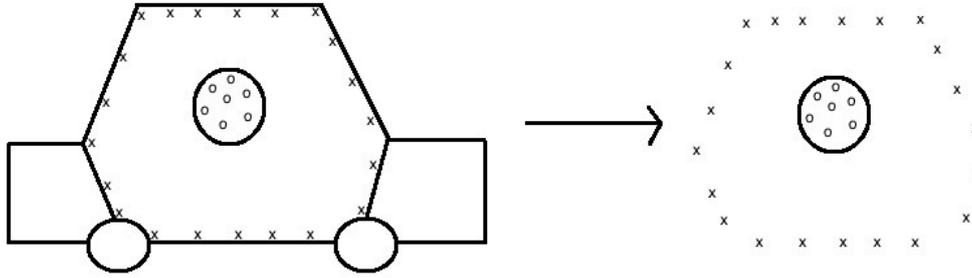

Figure 1: The measurements inside the car cabin is sketched to the left. During calculations an assumption of free field conditions is made, as sketched to the right. Circles represent microphones and crosses represent virtual sources.

Each elements in $\mathbf{H}$ is given by the relation between the volume velocities of the virtual sources distributed in a free field and the sound pressure they generate on a rigid sphere. This relation depends on the radius r, the inclination angle θ, and the azimuth angle φ. To simplify the calculations the coordinate system is rotated according to the position of each microphone placing it at $\theta = 0$, which makes the response independent of φ [3],

$$\left[H\left(r_j, \theta_i \right) \right] = -\frac{j\omega\rho}{2\pi a^2} \sum_{m=0}^{\infty} (m+0.5) \frac{h_m\left(kr_j\right)}{h'_m\left(kr_j\right)} P_m\left(\cos\theta_i\right), \tag{2}$$

where ω is the angular frequency, ρ the density of air, a is the radius of the sphere, r_j is the distance between the centre of the sphere and the virtual source, h_m and h'_m are the m'th order spherical Hankel function of the second kind and its derivative (not to be confused with the number of microphones), P_m is the Legendre polynomial of order m, and θ_i is the angle between the virtual source and microphone of interest.

The transfer matrix tends to smoothen the signal from the sources, as shown in Figure 2. The sources play at the same frequency, but with varying amplitudes (and phase angles) along θ as shown at the top of Figure 2. In the middle part of the figure the corresponding microphone pressures are shown when the sources play at 500 Hz, and in the bottom part the sound pressures at the microphones are shown when the sources play at 5000 Hz. At low frequencies the smoothing is more pronounced than at high frequencies because the sphere is smaller compared with the wavelength, and therefore the signal at 5000 Hz is much more fluctuating than at 500 Hz. Because of the high degree of smoothing at low

frequencies it is more difficult to reconstruct the source distribution in this frequency range than at higher frequencies where the smoothing is less pronounced.

To find the source distribution **q** on the car cabin from the measured microphone pressures **p**, the matrix **H** has to be inverted. This cannot be done directly, primarily because **H** has a high condition number in particular at low frequencies, which makes the inverse problem ill-posed and leads to the need for regularization.
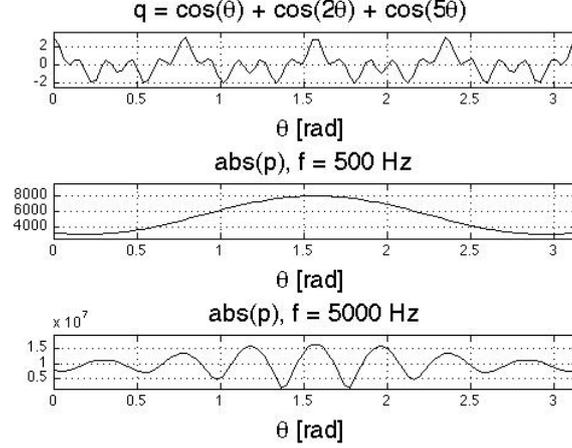

Figure 2: Top figure, varying source strengths; middle and bottom figure , resulting sound pressure over the sphere at two different frequencies.

2.2 Regularization

The regularizations used here are the Truncated Singular Value Decomposition (TSVD) and the Tikhonov regularization. Both modify the Singular Value Decomposition (SVD) of **H** [4],

$$\mathbf{H} = \mathbf{U}\mathbf{\Sigma}\mathbf{V}^{\mathrm{T}} = \sum_{i=1}^{m} u_i \sigma_i \upsilon_i^{\mathrm{T}} \tag{3}$$

where $\mathbf{U} = (u_1, u_2, \ldots, u_m)$ is an m by m orthogonal matrix, $\mathbf{V} = (v_1, v_2, \ldots, v_n)$ is an n by n orthogonal matrix, $\mathbf{\Sigma}$ is an m by n matrix, and T indicates the transpose. The elements in the diagonal are the singular values in decreasing order, $\sigma_1 \geq \sigma_2 \geq \ldots \geq \sigma_m \geq 0$. Because of the smoothing property of **H**, σ_1 corresponds to the lowest oscillation in the signal and σ_m corresponds to the highest oscillation.

The condition number of **H** is the relation between its largest and smallest singular value. Because the sphere is smoothing the signal more at low frequencies the difference between the largest and smallest singular value will be larger at low frequencies, which leads to a large condition number in this frequency range and a smaller one at high frequencies.

Using the SVD of **H** the pseudoinverse is [4]

$$\mathbf{H}^{\dagger} = \mathbf{V}\mathbf{\Sigma}^{\dagger}\mathbf{U}^{\mathrm{T}} = \sum_{i=1}^{rank(\mathbf{H})} \upsilon_i \sigma_i^{-1} u_i^{\mathrm{T}} \tag{4}$$

where $\mathbf{\Sigma}^{\dagger}$ is the pseudoinverse of $\mathbf{\Sigma}$ with elements of $1/\sigma_i$ in the diagonal, $0 \leq 1/\sigma_1 \leq 1/\sigma_2 \leq 1/\sigma_m$. The inversion of the elements in $\mathbf{\Sigma}$ means that high frequency oscillations in **p** are amplified much more than low frequency oscillations, which is consistent with the smoothing property of **H** in the direct problem. When noise is present in the problem this will mask the part of the signal corresponding to the small singular values. In the inverse problem these parts of the signal are the ones amplified the most, which means that the reconstruction will be completely masked by noise. By regularization it is possible to get meaningful results in the presence of noise.

Both the TSVD and Tikhonov regularizations can be seen as the addition of a filter factor, f_i, to Eq. (4). The filter factor determines the contribution from the i'th part of the sum to $\mathbf{H}^{\dagger}$. In both cases most weight is given to the largest singular

values. In TSVD the filter factors are either one or zero, which will leave the largest singular values unchanged and discard the smallest values contaminated with noise. In the Tikhonov regularization the filter factors are given by [5]

$$f_i = \frac{\sigma_i^2}{\sigma_i^2 + \lambda^2} \tag{5}$$

with λ being the regularization parameter. For singular values much larger than λ the filter factor is one and for singular values much smaller than λ the filter factor is zero. The transition between one and zero is smooth, whereas in the TSVD it is abrupt.

Discarding small singular values can be seen as a low pass filtering because the small singular values represent the oscillations of the highest frequencies in the signal. Only using low frequency oscillations in the reconstruction makes it impossible to reconstruct sharp edges, and the spatial resolution is decreased. The need for regularization is more pronounced at low frequencies because of to the larger condition number and more singular values are discarded from the measurements. This leads to a poorer resolution at low frequencies than at high frequencies.

The choice of regularization parameter is made using the *L*-curve and the generalized cross validation (GCV) [5].

3 Results

3.1 Simulations

Initially simulations with a point source have been made. To estimate the angular resolution of the method the source distribution was calculated on a sphere with a radius equal to the distance to the point source. The resolution is then determined as the angle between the source and the -3 dB point of the main lobe. The microphone array used for the simulations was chosen to be the same as in the measurements. It was an array with a radius of 9.75 cm and 50 microphones. The $m = 50$ microphones were evenly distributed on the sphere, which was a tilted version of the B&K spherical array Type 8606. The number of virtual sources was chosen as $n = 5000$. One of the virtual sources was chosen as a point source and the pressure distribution on the microphone array was calculated from the direct problem. Noise was added to **p**, and the source distribution was calculated from the inverse problem. The simulations were done with the TSVD and Tikhonov regularisation in combination with the *L*-curve and GCV methods to find the optimal regularization parameter. It was found that the Tikhonov regularisation in combination with the *L*-curve method worked best. The main problem with the TSVD is that the truncation parameter is discrete, which makes it more difficult to choose the right position on the curves for the two methods. If, however, the right regularization parameter was chosen, TSVD gave good results, but still they were not better than the ones obtained using Tikhonov regularization. Moreover, it was found that for the Tikhonov method the choice of regularization parameter was better using the *L*-curve than GCV. Therefore the solutions presented here are for the Tikhonov regularization in combination with the *L*-curve method.

The resolution at different distances to the spherical array and at different signal to noise ratios (SNR) is shown in Figure 3 and 4. It is seen that in general the resolution is best at high frequencies as expected.

In Figure 3 it is seen that the distance does not have a great impact on the resolution except when the source is very close to the microphone array. When the distance is 25 cm the angular resolution is around 40˚ up to 800 Hz. At distances between 50 cm and 210 cm the resolution is more or less the same in the range from 200 Hz to 800 Hz going from 65˚ to 40˚. Only at 100 Hz a major difference is seen: the resolution at 50 cm is 20˚ better than at 100 cm and 210 cm. Above 800 Hz the resolution is more or less the same independently of the distance to the source, going from 40˚ to around 27˚.

The spatial resolution is more influenced by the SNR. The resolution is found to depend on the SNR up to around 1500 Hz. At low SNRs the resolution is almost 200˚ at 100 Hz improving to a level of around 30˚ at 2000 Hz. At higher SNR values the resolution is 90˚ at 100 Hz and again improved to around 30˚ at 2000 Hz. At an SNR of 0 dB the reconstruction gives no meaningful result.
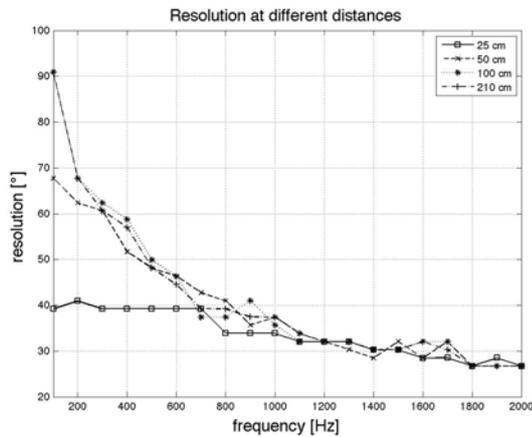
Figure 3: Resolution at distances 25 cm, 50 cm, 100 cm and 210 cm with an SNR of 30 dB.
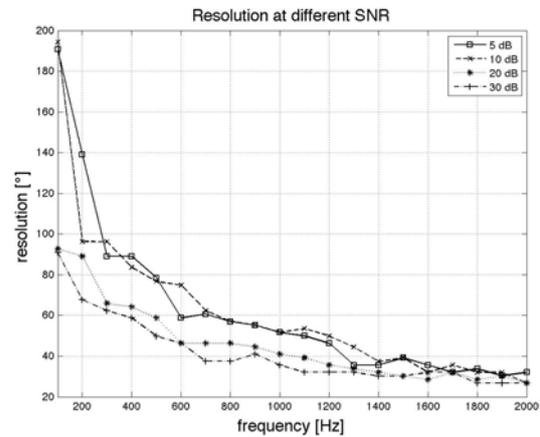

Figure 4: Resolution at SNRs of 5 dB, 10 dB, 20 dB and 30 dB at a distance of 1 m.

3.2 Experimental results

To check the model measurements have been performed under different conditions. Initially, a measurement was carried out in an anechoic room to make the conditions as close as possible to the assumed free field condition. Other measurements were taken inside a box made of wood with dimensions 122 cm by 172 cm by 122 cm. Some measurements were done with four out of six walls covered by 3 cm layer of absorbing material, and some with all six walls covered by 3 cm layer of absorbing material. The box setup was included to examine the influence on the result when measurements are made in environments with different degrees of reflections. In a real car some surfaces will be quite absorbing and others will be highly reflective.

The microphone array used in the anechoic room was a spherical array with a radius of 9.75 cm and 36 microphones. The microphone array used in the box had the same radius but 50 microphones with the same positions as used in the simulations. The distance from the array to the source was 210 cm in the anechoic room and 75 cm in the box. The loudspeaker source was driven with broad band random noise, and the contribution at each frequency was found by measuring cross power spectral densities with microphone 1 used as a reference.

The calculated spatial resolutions are shown in Figure 5. It is seen that the resolution is quite good in the anechoic room starting at 50˚ at 100 Hz and improving to less than 20˚ at 2000 Hz. The resolution in the box is less impressive, but more or less the same in the case with all walls covered by panels and in the case when four walls are covered by panels. Here the resolution starts at 150˚ at 100 Hz and improves to 30˚ at 2000 Hz.
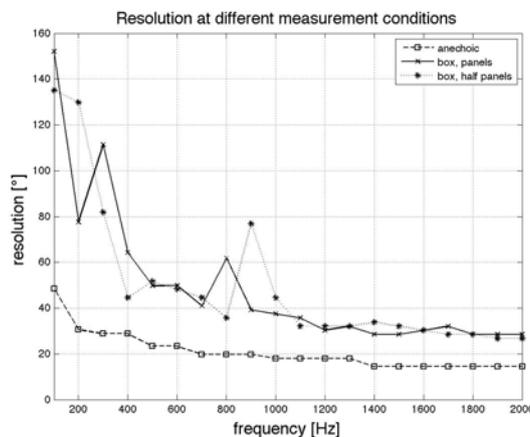

Figure 5: Spatial resolution in measurements in the anechoic room and in the box under two different conditions.

4   Discussion

Simulations and measurements show that the inverse method can be used for noise localization. The resolution is dependent on the SNR and to some extent also on the distance from the microphone array to the source. The measurement in the anechoic room is better than expected from the simulations, whereas the box measurements are somewhat worse than simulations. It was expected that worse results should obtained in the box than in simulations since the model is based on an assumption of free field conditions. This assumption is not fulfilled in the box where the boundary conditions at the walls optimally should be taken into account in the calculation of the elements of **H**. Still, the source is localized quite well as long as damping material is introduced at some of the walls. Comparable conditions are found in a car where the seats will have a damping effect whereas the doors and windows will reflect the sound.

The results have been compared to the results obtained by Jourdan and Marschall [6], where simulations and measurements were made using spherical harmonics beamforming. Jourdan and Marschall used a spherical array with a radius of 14 cm and 64 microphones and a distance to the source of 1.2 m.

The resolution decreases stepwise when spherical harmonics beamforming is used, which means that the resolution is the same from 200 Hz to 600 Hz and again from 600 Hz to 1000 Hz. This gives the solution using the inverse problem an advantage in the simulations at all frequencies in these ranges, except at 200 Hz and 600 Hz where the resolution is more or less the same using the two methods. At frequencies above 1000 Hz there are no major differences in the resolution. Comparing measurements from the anechoic rooms, the inverse transfer matrix method presented here has an advantage over spherical harmonics beamforming in the entire frequency range from 200 Hz to 2000 Hz.

5   Conclusions

It has been demonstrated that the inverse transfer matrix method can be used for localization of sound sources in an environment similar to that in a car. In simulations and measurements in an anechoic room a point source can be localised from measured microphone pressures on a spherical array. The spatial resolution at 100 Hz is found to be 50˚ and improving to less than 20˚ at 2000 Hz when measurements are done in an anechoic room. Measurements from a box made of wood show results somewhat worse, but the source can still be localized as long as some of the walls are covered by absorbing material. Comparing the results to results from the literature using spherical harmonics beamforming, the method presented in this paper was found to give better spatial resolution at low frequencies, but at higher frequencies the resolution was the same for the two methods.

6   Future work

Now that it has been demonstrated that the method works under different conditions, measurements can be made in a real car. The measurements should be done with a controlled source as a start to check whether the environment in the car will give too many reflections for the method to work. Afterwards the method will be examined with the engine running.

Other measurements could investigate the difference between results when sources are correlated and uncorrelated. In a car with reflecting surfaces many sources will be correlated, and therefore it is instructive to see whether the method has the same performance when the sources are correlated and uncorrelated.

References

[1]   L. Lamotte, M. Robin and F. Deblauwe, Noise mapping and sound quantification in the space using spherical array, *Proceedings of Euronoise 2009*, Edinburgh, Scotland, 2009.

[2]   Q. Leclere, Acoustic imaging using under-determined inverse approaches: Frequency limitations and optimal regularization, *Journal of Sound and Vibration* **321**, 2009, 605-619.

[3]   F. Jacobsen and P. Juhl, Radiation of Sound, DTU, Lyngby, 2010.

[4]   G. Strang, The Fundamental Theorem of Linear Algebra, *The American Monthly*, Vol. 100, No 9, 1993, 848-855.

[5]   P. C. Hansen, Rank-Deficient and Discrete Ill-Posed Problems, *Siam*, USA, 1998.

[6]   J. Jourdan and M. Marschall, Comparison of Beamforming Techniques on a Sphere, DTU, Lyngby, 2008.